J Mater Sci (2015) 50:7627–7635
DOI 10.1007/s10853-015-9325-1

# Structures and properties of diamond-like phases derived from carbon nanotubes and three-dimensional graphites

**E. A. Belenkov[1] · V. A. Greshnyakov[1]**

Received: 13 May 2015 / Accepted: 1 August 2015 / Published online: 20 August 2015


**Abstract** A theoretical analysis of structures of diamond-like phases which are obtained from single-walled carbon nanotubes and three-dimensional graphites is performed. As a result of the analysis, the possibility of stable existence of thirteen phases in which carbon atoms are in crystallographically equivalent positions is established. We have found two novel chiral phases, precursors of which are three-dimensional graphites. Using the density functional theory method in the generalized gradient approximation, geometrically optimized structures for all phases are calculated, as well as cohesive energies, electron densities of states, bulk moduli, hardness, and X-ray powder diffraction patterns. The chemical composition of diamond-like phases is identical; however, their properties vary within wide ranges.

## Introduction

Diamond-like phases consist of carbon atoms in four-coordinated states [1]. The number of diamond-like structures consisting of atoms in crystallographically equivalent positions should be finite similar to the limited number of two-dimensional uninodal nets. So the number of the flat two-dimensional nets formed by equivalent three-coordinated nodes is equal to four [2]. The problem of describing all possible three-dimensional nets of four-coordinated atoms and related diamond-like phases has not been solved yet. As a possible method of describing diamond-like phases in which all atoms are in equivalent positions, it is possible to use a model scheme for obtaining their structures from precursors of three-coordinated atoms [3]. For obtaining diamond-like phases with equivalent positions of atoms, precursors should also consist of equivalent atoms. The number of such structural precursors is finite, and it is possible to consider them all in detail and then obtain a full set of diamond-like nets. These precursors relate to four main structural groups [$0D_c$, 3], [$1D_c$, 3], [$2D_c$, 3], and [$3D_c$, 3] typical representatives of which are fullerenes, carbon nanotubes, graphene layers, and three-dimensional (3D) graphites, respectively [3]. Of special interest are diamond-like phases which can be obtained from nanotubes and 3D-graphites.

Carbon nanotubes (CNTs) are cylindrical frame nanostructures formed by rolling graphene sheets. Carbon atoms in the nanotube structure are in three-coordinated states ($sp^2$ hybridization). The early reports about a synthesis of CNTs were made in [4, 5]. However, nanotubes became widely known after Sumio Iijima's observations [6]. The interest in nanotubes is connected with the possibility of their practical application in electronics, materials science, medicine, and chemical technologies. In materials science, CNTs can be used as initial materials for the synthesis of diamond and diamond-like phases. This is related that carbon atoms in nanotubes are on the surface of strongly curved graphene layers in a hybridization state which is intermediate between the hybridization of atoms in graphene and diamond. Therefore, it is possible to synthesize diamond-like phases from nanotubes under lower pressures and temperatures than from graphite.

Cubic diamond (*c*-diamond) was experimentally obtained from CNTs under 4.5 GPa and 1300 °C in the presence of Ni/Mn/Co catalysts [7]. In [8], diamond was synthesized from multi-walled nanotubes under 80 GPa and 1500 °C. Lonsdaleite (2*H* diamond polytype) was

✉ E. A. Belenkov
belenkov@csu.ru

[1] Chelyabinsk State University, Chelyabinsk, Russia

obtained by compressing ($P = 9$ GPa) a nanotube bundle under a temperature of 700 °C in the presence of Ni/Co catalysts [9]. By changing pressures, temperatures, and catalysts, it is possible to obtain a number of diamond-like and hybrid phases from CNTs [10–13].

In [14–19], some theoretical investigations of the process of obtaining compounds with diamond-like structures from CNTs were performed. Diamond-like phases can be derived by linking of zigzag ($n$, 0) single-walled carbon nanotube (SWCNTs) bundles, where $n = 2, 3, 4, 6$ [14–16]. Moreover, diamond-like phases can be obtained from armchair ($m$, $m$) single-walled nanotubes, where $m = 2, 3, 4, 6, 8, 10$ [14–19].

One more new class of structural precursors for obtaining diamond-like phases is represented by 3D-graphites, which are just a subject of theoretical investigations yet. Three-dimensional graphites are phases of three-dimensional covalent bonded three-coordinated ($sp^2$) carbon atoms. From the 3D-graphites, diamond-like structures can be theoretically obtained by linking three-coordinated neighboring atoms, as a result of which atoms converse into a four-coordinated state [2, 20]. The 3D-graphites should consist of atoms which are in crystallographically equivalent positions. To date, only thirteen such $sp^2$ phases have been studied in detail: *bct*-4 ($I4_1/amd$), $C_1$ $3_1$ ($P6_222$), $C_1$ $4_1$ ($K4$, $I4_132$), $C_2$ 4 (*bct*-8, $I4_1/amd$), $C_2$ 3 ($R6$, $R\bar{3}m$), $H$-6 ($P6_222$), $6.8^2$ $P$ ($Im\bar{3}m$), $6.8^2$ $D$ ($Pn\bar{3}m$), $6.8^2$ $G$ ($Ia\bar{3}d$), 6(3)1-06 ($P6_222$), $sp^2$-diamond ($Fd\bar{3}m$), 206-48$e$ ($Ia\bar{3}$), and 6(3)1–10 ($rh6$, $R\bar{3}m$).

In this paper, we demonstrate the results of the theoretical analysis of the possible structures and properties of carbon diamond-like phases with equivalent crystallographic atomic positions, which are obtained by linking or combining nanotubes and as a result of internally linking 3D-graphites.

## Method

To construct the structures of diamond-like tubulane phases (called $T$-phases), some carbon nanotubes ($n$, $m$) from the structural group [$1D_c$, 3] are used whose sum of indexes ($n + m$) does not exceed six. This restriction follows from the limit of the number of nanotube edges, while linking or combining of which can form 3-coordinated regular graphs of the structural group [$2D_c$, 3] in the projection onto the 001 plane. From three-dimensional graphites of the structural group [$3D_c$, 3], spiral diamond-like phases (called $S$-phases) can also be obtained. In the present paper, four previously investigated 3D-graphites are considered as precursors of diamond-like phases: $C_1$ $3_1$ (Fig. 1a), $K4$ (Fig. 1b), $H$-6 (Fig. 1c), and $rh6$ (Fig. 1d). The choice of a

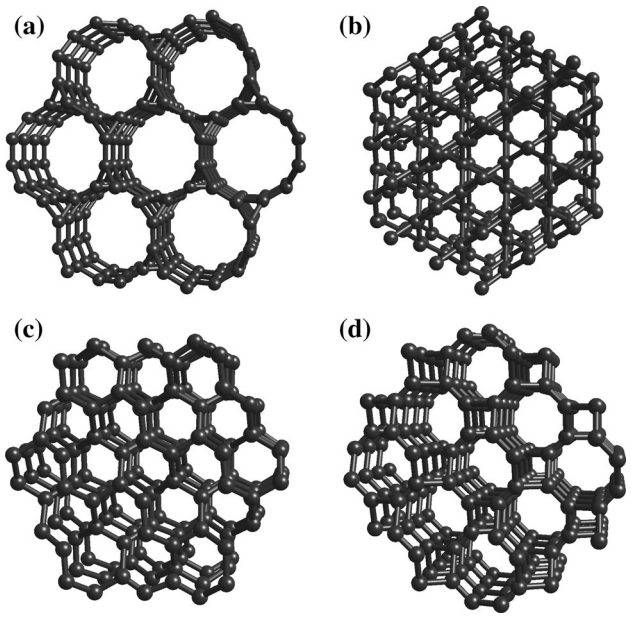


**Fig. 1** The crystal structures of $C_1$ $3_1$ (**a**), $K4$ (**b**), $H$-6 (**c**), and $rh6$ (**d**) 3D-graphites

limited number of 3D-graphites was determined that new diamond-like phases are only derived from these precursors. In diamond-like phase notation, symbols "$T$" and "$S$" characterize a group of precursors (CNTs and 3D-graphites, respectively). Further, the phase name has the phase number and a symbol indicating the method of obtaining the phase from precursors ("$A$" is linking; "$B$" is combining) [20].

The structures, energy characteristics, and electronic properties of diamond-like phases were calculated in the Quantum ESPRESSO software package [21] using the density functional theory (DFT) method within the generalized gradient approximation (GGA), with a B3LYP hybrid exchange-correlation functional [22]. Norm-conserving pseudopotentials are employed in conjunction with plane-wave basis sets of a cutoff energy of 60 Ryd and $12 \times 12 \times 12$ Monkhorst–Pack Brillouin-zone $k$-point grids. The bulk moduli of diamond-like phases are calculated using a technique which was proposed in [23]. The absolute values of atomic volumes and total energies, necessary for defining the bulk moduli, were calculated by the GGA-DFT method. The Vickers hardness of carbon compounds was calculated by the Gao's hardness model [24]. The Knoop hardness was also determined according to the Li's method [25]. The standard method [26] for calculating the powder X-ray diffraction (XRD) patterns was used. Interatomic bond lengths and angles between them were found for every diamond-like phase. Based on these, deformation *Def* and *Str* parameters are calculated which characterize the stress of the phase structure relative

to that of cubic diamond as the most stable carbon polymorph of four-coordinated atoms. The *Def* parameter represents the sum of moduli of the bond angle deviation from diamond angle 109.47° [20]. The *Str* deformation parameter is calculated as the sum of moduli of the difference of interatomic bond lengths in the phase and diamond [27].

## Results and discussion

The theoretical analysis and model calculations showed the possibility of existence of ten diamond-like *T*-phases and four *S*-phases. Figure 2 pictures the crystal structures of these phases. The *TA*1–*TA*8 phases were obtained by linking of armchair or zigzag SWCNTs, while *TB* can only be obtained in the process of combining nanotubes. The structures of diamond-like *S*-phases are only formed by internally linking 3D-graphites. Note that each of the four *S*-phases has two enantiomorphous versions (Table 1).

Precursors, space groups, unit cell parameters, and ring parameters (Wells' parameter) of cubic diamond and diamond-like phases are shown in Table 1. Table 1 also displays types of four-coordinated zeolite nets corresponding to the carbon diamond-like phases. The ring parameter shows that nine *T*-phases and three *S*-phases contain rings of six carbon atoms; *SA*4 and eight *T*-phases contain 4-membered rings; rings of eight atoms are observed in four *T*-phases and two *S*-phases; 3-, 5-, and 10-membered rings found only in *TB*, *SA*1, and *SA*4 phases, respectively.

For any diamond-like phase, the deformation parameter *Def* and *Str* values are larger than zero: *Def* $\in$ [34.87°; 95.40°] and *Str* $\in$ [0.038 Å; 0.290 Å] for *T*- and *S*-phases (Table 2). The calculated densities of diamond-like phases are given in Table 2. The *TA*4 phase has the minimum density (less than $\rho_{\text{diamond}}$ by 24.6 %), and the maximum density corresponds to *SA*2 phase (it exceeds $\rho_{\text{diamond}}$ by 3.7 %).

Table 2 also presents the calculated cohesive energies ($E_{\text{coh}}$) and the differential total energies of *T*- and *S*-phases relative to those of cubic diamond ($\Delta E_{\text{diam}}$). The calculated cohesive energy of cubic diamond agrees completely with the corresponding experimental energy (7.37 eV/atom [28]). The total energies of all diamond-like phases exceed the diamond energy by the value ranging from 0.12 eV/atom (*SA*1) to 1.17 eV/atom (*SA*2). The diamond-like phase cohesive energy decreases linearly with increasing a linear combination of deformation *Def* and *Str* parameters. The *TA*6 and *SA*1 phases should be the most stable diamond-like phases since their cohesive energies are less than those of cubic diamond not more than by 4.4 %. Other phases have cohesive energy values lower than those of diamond by 4.7–14.9 %. However, the *TA*1–*TA*5, *TA*7–*TB*, and *SA*3 phases can also be stable under standard conditions since one diamond-like phase, *LA*4 ($C_8$), having a cohesive energy by 9.5 % less than that of cubic diamond [27], was synthesized and stably exists under standard conditions [29].

The electron densities of states of diamond-like phases are shown in Fig. 3. The calculated value of the electronic band gap in diamond was 5.44 eV (Table 3; Fig. 3a) and is in good agreement with the experimental value of 5.48 eV [28]. The band gaps of *T*-and *S*-phases were also determined from the calculated DOS (Table 2). It was found that the band gaps for diamond-like phases are less than those in cubic diamond with the value from 0.56 to 4.13 eV. The band gap decreases with the discrete increase of *Str*.

We also calculated the bulk modulus ($B_0$) and the Vickers ($H_V$) and Knoop ($H_K$) hardness of diamond-like phases as listed in Table 2. The calculated bulk modulus (445.1 GPa) and the Vickers and Knoop hardness (90.0 and 86.6 GPa, respectively) of cubic diamond agree well with the corresponding experimental values (443 [28], 96 [30], and 90 GPa [31], respectively). The bulk modulus values of *T*- and *S*-phases are smaller than those of diamond by the value in the range from 1.5 (*SA*2) to 31 % (*TA*4). The bulk modulus is found to be directly proportional to the diamond-like phase density: $B_0 \propto \rho$. The calculations showed that dense *SA*1–*SA*4 and *TA*6 phases have the maximum hardness.

For the possibility to experimentally identify new diamond polymorphs, powder XRD patterns were calculated (Table 4). These patterns were compared with the experimental diffraction patterns of cubic diamond, lonsdaleite, and hexagonal (2*H*) graphite. The first and second diffraction maxima of *SA*3 phase are close to the main maximum of cubic diamond ($2\theta_{111} = 43.91°$ [32]), to the second 100 %-maximum of lonsdaleite ($2\theta_{002} = 43.9°$ [33]), and to the 6 %-maximum of 2*H* graphite ($2\theta_{101} = 44.39°$ [34]). For *SA*4 phase, the 100 %-peak is close to the most intensive (002) peak of hexagonal graphite. For other phases in comparison with diamond, 2*H* graphite, or lonsdaleite, either the angular divergence in peak positions ($\Delta 2\theta$) exceeds 0.8°, or the phase peaks overlap with maxima whose intensity is less than 24 %.

The presence structural units of diamond-like phases available in experimentally obtained hydrocarbons indicates the probable thermodynamic stability of these phases. For example, four-membered rings with common sides, which are structural units of the *TA*1, *TA*2, *TA*4, and *TA*5 phases, are contained in ladderanes [35], prismane [36], cubane [37], pentaprismane [38], and pentacyclic propellene [39]. The *TA*3 and *TA*6-*TA*8 phases consist of carbon frames of polymerized cyclobutane rings, whereas the *TB* phase contains cyclopropane carbon frames. Double tetraasterane [40] is a structural motif of the *TA*8 phase.

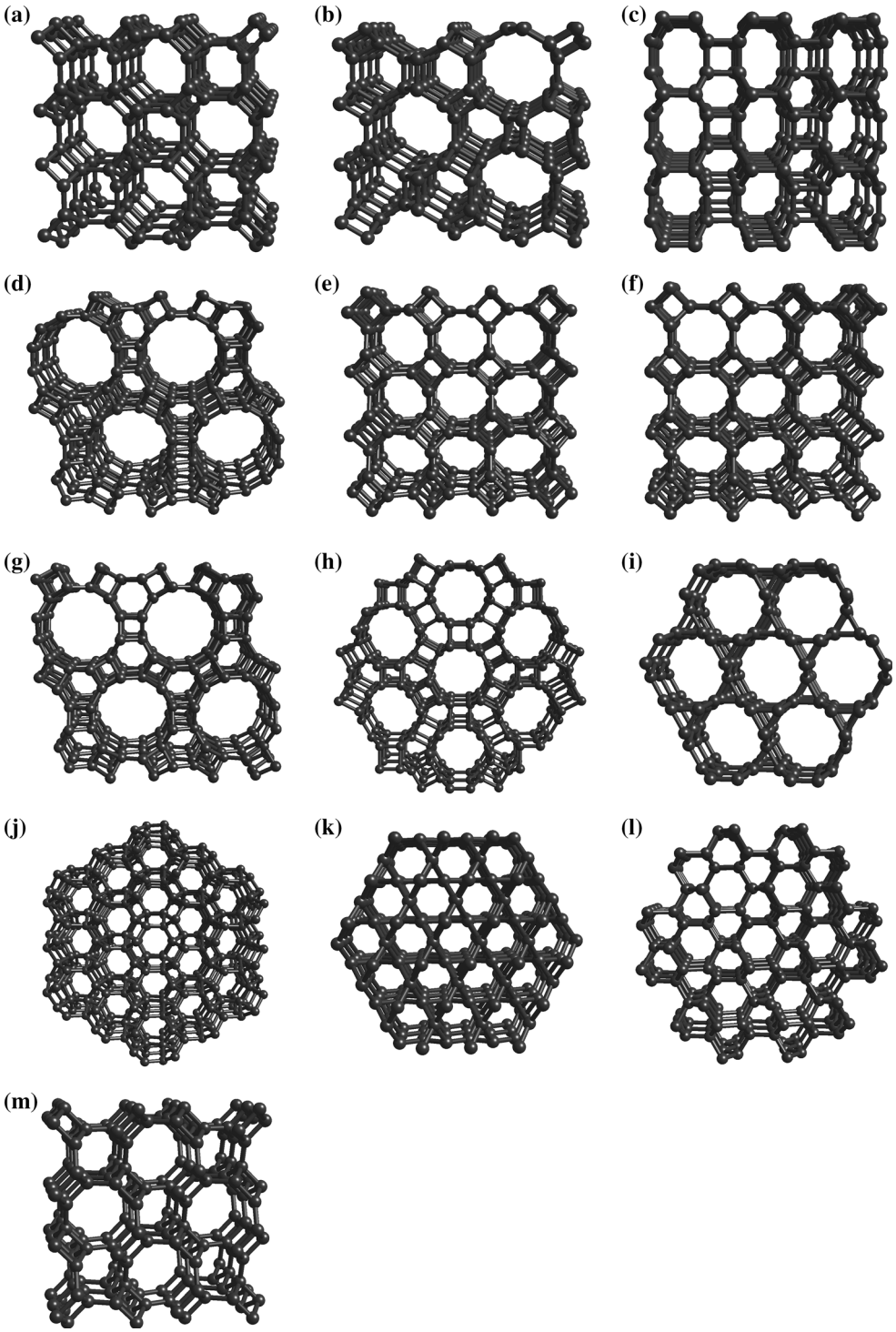


**Fig. 2** Fragments of the geometrically optimized structures of the following diamond-like phases: *TA*1 (**a**), *TA*2 (**b**), *TA*3 (**c**), *TA*4 (**d**), *TA*5 (**e**), *TA*6 (**f**), *TA*7 (**g**), *TA*8 (**h**), *TB* (**i**), *SA*1 (**j**), *SA*2 (**k**), *SA*3 (**l**), and *SA*4 (**m**)

The spiral *SA*1 phase structure has units shaped as half the dodecahedrane molecule [41]. All of the considered saturated hydrocarbon molecules are stable under standard conditions which make possible the stable existence of diamond-like phases on their basis.

The existence of the $sp^2$ precursor structures supports the plausibility that the diamond-like phases could be formed by their polymerization. Graphene layers [42] and small-diameter (2, 2) [43], (3, 3) [44], (4, 0) [45], and (6, 0) [46] SWCNTs relate to such precursors which stably exist under standard conditions. Polymerization of these precursors makes it possible to experimentally obtain the following phases: *TA*6, *TA*7, and *TA*8 (from graphene layers); *TA*1 (from (2, 2) nanotubes); *TA*2 and *TA*8 (from

**Table 1** Precursors, space groups, unit cell characteristics, ring parameters, and types of analogous zeolitic nets for cubic diamond and diamond-like phases

| Phase | Precursor | Space group | $a$ (Å) | $c$ (Å) | $Z$ (at.) | Ring parameter | Zeolite analog |
|---|---|---|---|---|---|---|---|
| *c*-diamond | Graphene $L_6$ | $Fd\bar{3}m$ | 3.597[a] | 3.597 | 8 | $6^6$ | – |
| *bct* $C_4$ | Graphene $L_6$ | *I*4/*mmm* | 4.401[a] | 2.525[a] | 8 | $4^1 6^5$ | BCT |
| *TA*1 | CNT (2, 2) | *I*4/*mmm* | 6.591 | 2.546 | 16 | $4^2 6^3 8^1$ | ATN |
| *TA*2 | CNT (3, 3) | $P6_3/mmc$ | 6.147 | 2.574 | 12 | $4^2 6^4$ | CAN |
| *TA*3 | CNT (2, 0) | $P4_2/mmc$ | 3.586 | 4.353 | 8 | $4^2 6^2 8^2$ | DFT |
| *TA*4 | CNT (3, 0) | $P6_3/mmc$ | 6.987 | 4.381 | 24 | $4^2 6^3 8^1$ | – |
| *TA*5 | CNT (4, 0) | *I*4/*mcm* | 7.079 | 4.412 | 32 | $4^2 6^3 8^1$ | MER |
| *TA*6 | CNT (4, 0) | *I*4/*mcm* | 4.969 | 4.215 | 16 | $4^1 6^5$ | – |
| *TA*7 | CNT (6, 0) | *P*6/*mcc* | 6.888 | 4.218 | 24 | $4^1 6^5$ | AFI |
| *TA*8 | CNT (3, 3) | $R\bar{3}m$ | 10.582 | 2.511 | 36 | $4^1 6^5$ | ATO |
| *TB* | CNT (3, 3) | $P6_3/mmc$ | 4.489 | 2.545 | 6 | $3^1 6^5$ | NPO |
| *SA*1 | $C_1$ $3_1$ | $P6_122$ ($P6_522$) | 3.584 | 3.397 | 6 | $5^5 8^1$ | – |
| *SA*2 | *H*-6 | $P6_222$ ($P6_422$) | 2.621 | 2.830 | 3 | $6^4 8^2$ | – |
| *SA*3 | 6(3)1-06 | $P6_122$ ($P6_522$) | 4.070 | 2.478 | 6 | $6^5 8^1$ | – |
| *SA*4 | *K*4 | $P4_122$ ($P4_322$) | 4.685 | 2.545 | 8 | $4^2 6^3 10^1$ | – |

[a] Reference [27]

**Table 2** Deformation parameters (*Def* and *Str*), densities ($\rho$), cohesive energies ($E_{coh}$), differential total energies ($\Delta E_{diam}$), band gaps ($\Delta$), bulk moduli ($B_0$), and hardness ($H_V$ and $H_K$) of cubic diamond and diamond-like phases

| Phase | *Def* (°) | *Str* (Å) | $\rho$ (g/cm$^3$) | $E_{coh}$ (eV/atom) | $\Delta E_{diam}$ (eV/atom) | $\Delta$ (eV) | $B_0$ (GPa) | $H_V$ (GPa) | $H_K$ (GPa) |
|---|---|---|---|---|---|---|---|---|---|
| *c*-diamond (calc) | 0.00 | 0.000 | 3.428[a] | 7.86[a] | 0.00 | 5.43 | 445.1 | 90.0 | 86.6 |
| *c*-diamond (exp) | – | – | 3.516[b] | 7.37[b] | – | 5.48[b] | 443[b] | 96[c] | 90[d] |
| *bct* $C_4$ | 37.55[a] | 0.110[a] | 3.262[a] | 7.64[a] | 0.21 | 4.30[a] | 439.9 | 86.8 | 82.1 |
| *TA*1 | 73.83 | 0.081 | 2.886 | 7.32 | 0.53 | 1.31 | 356.6 | 79.8 | 72.2 |
| *TA*2 | 70.96 | 0.130 | 2.842 | 7.40 | 0.46 | 3.28 | 343.9 | 79.1 | 71.1 |
| *TA*3 | 95.40 | 0.066 | 2.851 | 7.18 | 0.68 | 2.48 | 337.7 | 78.9 | 71.2 |
| *TA*4 | 83.92 | 0.133 | 2.585 | 7.16 | 0.69 | 4.62 | 306.2 | 73.4 | 64.0 |
| *TA*5 | 74.23 | 0.121 | 2.887 | 7.37 | 0.49 | 3.59 | 336.5 | 78.8 | 71.8 |
| *TA*6 | 49.50 | 0.117 | 3.067 | 7.51 | 0.35 | 4.16 | 372.7 | 83.1 | 76.9 |
| *TA*7 | 49.79 | 0.124 | 2.762 | 7.38 | 0.47 | 3.80 | 319.5 | 77.0 | 68.7 |
| *TA*8 | 60.27 | 0.232 | 2.949 | 7.27 | 0.58 | 3.10 | 353.9 | 78.8 | 73.0 |
| *TB* | 88.09 | 0.129 | 2.694 | 7.49 | 0.36 | 2.63 | 348.7 | 80.8 | 68.8 |
| *SA*1 | 34.87 | 0.038 | 3.167 | 7.73 | 0.12 | 4.88 | 392.2 | 85.2 | 79.7 |
| *SA*2 | 84.80 | 0.228 | 3.554 | 6.69 | 1.17 | 2.59 | 438.3 | 84.3 | 86.6 |
| *SA*3 | 66.80 | 0.121 | 3.367 | 7.14 | 0.72 | 3.16 | 425.9 | 84.8 | 83.3 |
| *SA*4 | 84.56 | 0.290 | 3.298 | 6.74 | 1.12 | 2.57 | 341.3 | 82.6 | 81.1 |

[a] Reference [27]

[b] Reference [28]

[c] Reference [30]

[d] Reference [31]

(3, 3) CNTs); *TA*5 and *TA*6 (from (4, 0) CNTs); and *TA*7 (from (6, 0) CNTs).

Some possible methods for synthesizing diamond-like phases from various precursors are given in Table 4. An analysis showed that the main method for obtaining the majority of *T*-phases is linking. This process can be experimentally realized under strong compression of single-walled or double-walled carbon nanotube bundles in the directions perpendicular to nanotube axes. To provide the irreversible formation of covalent bonds between

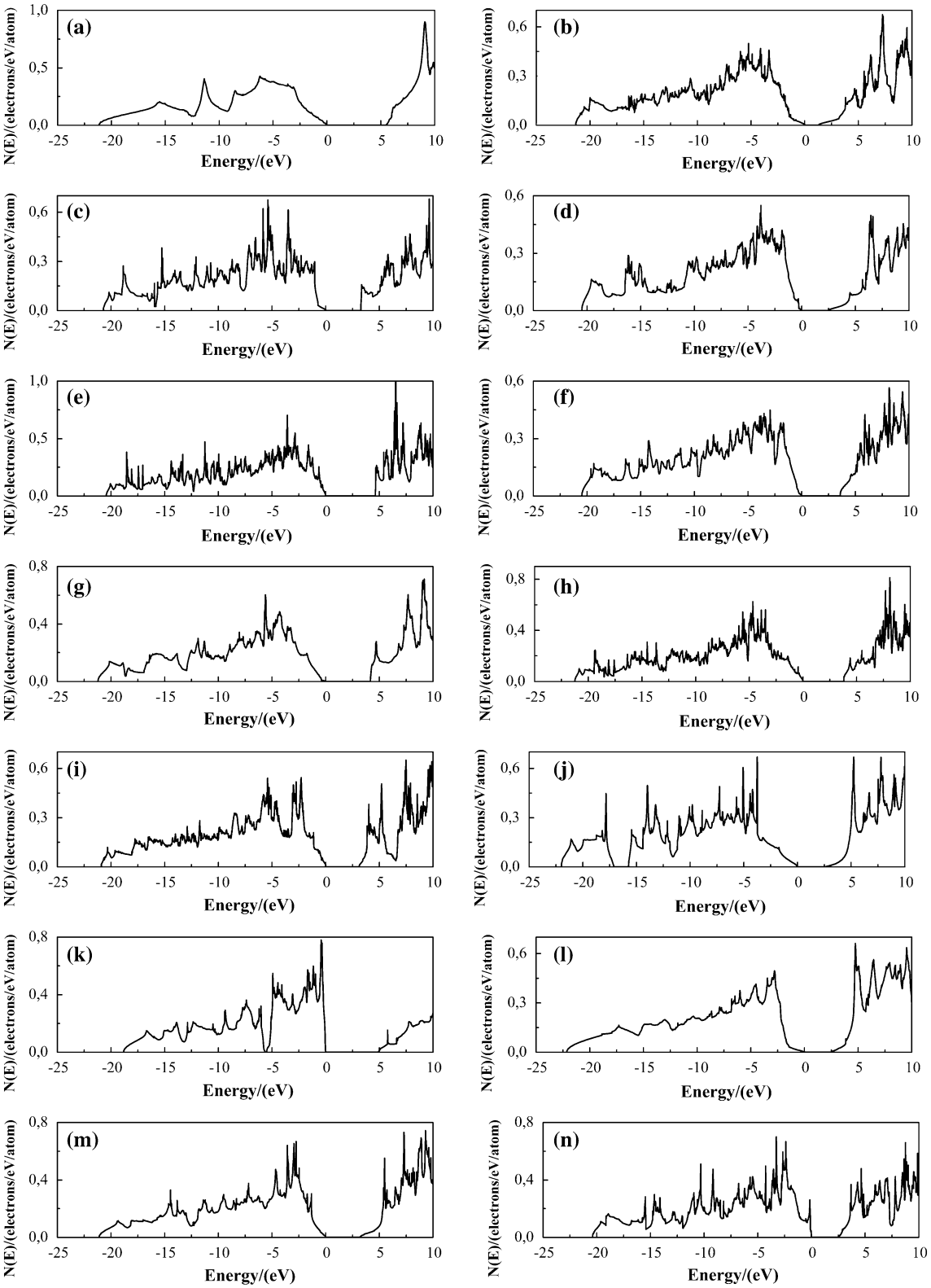


**Fig. 3** Densities of electronic states of the *LA*1 (**a**), *TA*1 (**b**), *TA*2 (**c**), *TA*3 (**d**), *TA*4 (**e**), *TA*5 (**f**), *TA*6 (**g**), *TA*7 (**h**), *TA*8 (**i**), *TB* (**j**), *SA*1 (**k**), *SA*2 (**l**), *SA*3 (**m**), and *SA*4 (**n**) phases (the valence band maximum is set to zero on the energy scale)

**Table 3** Diffraction maxima of the highest intensity for cubic diamond, lonsdaleite, 2*H* graphite, and diamond-like phases

| Phase | $d_1$/(Å) | $I_1$/(%) | $d_2$/(Å) | $I_2$/(%) | $d_3$/(Å) | $I_3$/(%) |
|---|---|---|---|---|---|---|
| *c*-diamond (exp)[a] | 2.060 | 100 | 1.261 | 25 | 1.0754 | 16 |
| Lonsdaleite (exp)[b] | 2.19 | 100 | 2.06 | 100 | 1.26 | 75 |
| 2*H* graphite (exp)[c] | 3.376 | 100 | 2.039 | 6 | 1.6811 | 4 |
| *TA*1 | 3.295 | 100 | 4.660 | 88.8 | 1.9265 | 32.7 |
| *TA*2 | 5.323 | 100 | 3.073 | 58.4 | 2.3173 | 21.9 |
| *TA*3 | 3.586 | 100 | 2.768 | 28.6 | 2.1763 | 17.4 |
| *TA*4 | 6.051 | 100 | 2.2869 | 2.9 | 2.1904 | 2.7 |
| *TA*5 | 3.539 | 100 | 2.572 | 35.1 | 2.2061 | 24.4 |
| *TA*6 | 3.514 | 100 | 1.9657 | 26.2 | 2.1073 | 22.9 |
| *TA*7 | 5.965 | 100 | 1.9884 | 3.9 | 3.444 | 3.6 |
| *TA*8 | 5.291 | 100 | 1.9998 | 14.2 | 2.2019 | 13.5 |
| *TB* | 3.888 | 100 | 2.1294 | 20.3 | 1.9439 | 14.8 |
| *SA*1 | 2.291 | 100 | 3.104 | 69.9 | 1.5849 | 12.2 |
| *SA*2 | 1.7707 | 100 | 2.270 | 36.6 | 1.2008 | 18.2 |
| *SA*3 | 2.0267 | 100 | 3.523 | 88.2 | 2.0338 | 71.7 |
| *SA*4 | 3.313 | 100 | 4.685 | 68.8 | 2.236 | 37.4 |

$\lambda_{\text{Cu-}\alpha} = 1.5405$ Å

[a] Reference [32]

[b] Reference [33]

[c] Reference [34]

**Table 4** Possible methods for the synthesis of diamond-like phases from precursors (synthetic routes: 1—polymerization of a condensate under high pressure; 2 and 3—polymerization of saturated or nonsaturated hydrocarbons, respectively)

| Phase | Precursors | Synthetic route |
|---|---|---|
| *TA*1 | (2, 2)/(8, 8)/$L_{4-8}$ graphene | 1 |
| | Ladderanes | 2 |
| | Dimeric cyclo-octatetraene/tricyclo[4.2.2.2$^{2,5}$]dodeca-1,5-diene | 3 |
| *TA*2 | (3, 3)/(3, 3)@(9, 9)/$L_{4-6-12}$ | 1 |
| | Ladderanes | 2 |
| | Didehydrobiphenylenes/tetracyclo[8.2.2.2$^{2,5}$.2$^{6,9}$]-1,5,9-octadecatriene | 3 |
| *TA*3 | (2, 0)/$L_{4-8}$ | 1 |
| | Cyclobutadiene/dimeric cyclo-octatetraene | 3 |
| *TA*4 | (2, 0)/(3, 0)/$L_{4-6-12}$ | 1 |
| | Didehydrobiphenylenes | 3 |
| *TA*5 | (4, 0)/$L_{4-8}$ | 1 |
| | Dimeric cyclo-octatetraene | 3 |
| *TA*6 | (4, 0)/(4, 0)@(12, 0)/(8, 0)@(16, 0)/$L_6$/$L_{4-8}$ | 1 |
| | Dimeric cyclo-octatetraene | 3 |
| *TA*7 | (2, 0)/(3, 0)/(6, 0)/(6, 0)@(18, 0)/$L_6$/$L_{4-6-12}$ | 1 |
| | Didehydrobiphenylenes | 3 |
| *TA*8 | (2, 1)/(3, 3)/$L_6$/$L_{4-6-12}$ | 1 |
| | Tetraasteranes | 2 |
| | Didehydrobiphenylenes/tetracyclo[8.2.2.2$^{2,5}$.2$^{6,9}$]-1,5,9-octadecatriene | 3 |
| *TB* | "Sandwich" packing of $L_6$ and carbyne chains/$L_{3-12}$ | 1 |
| *SA*1 | Dense hexagonal bundle of carbyne chains | 1 |
| *SA*2 | Dense hexagonal bundle of carbyne chains | 1 |
| *SA*3 | (2, 1)/"sandwich" packing of $L_6$ and carbyne chains/dense hexagonal bundle of carbyne chains | 1 |
| *SA*4 | (3, 1)/(5, 3)/incompact tetragonal bundle of carbyne chains | 1 |

nanotube walls, the pressure value should exceed 24 GPa [10, 11] because it is only possible to observe the appearance of nanotube wall faceting at lower pressures [47]. As the theoretical calculations showed [16, 17, 48], an increase in the nanotube surface curvature leads to a decrease in the pressure value necessary for wall polymerization. Therefore, it is more preferable to use nanotubes with minimum diameters (i.e., with minimum chirality indices) for the synthesis of new diamond-like phases.

The electronic bombardment of the initial fullerite or CNT bundle is one more influence method which can result in the formation of covalent bonds between walls of nanotubes [49]. It is also possible to irradiate nanotube bundles using ion beams so that covalent bonds are formed, but in this case initial CNTs can be considerably damaged by the ion beam influence [50].

The *TA*6, *TA*7, and *TA*8 phases can be probably obtained by compressing graphite crystals in the pressure range of $P > 15$ GPa in which transparent hybrid carbon compounds are observed [51]. Except for CNTs or graphene layers, diamond-like phases can be obtained from hydrocarbon molecules. Initial molecules should have a carbon frame similar to structural units of diamond-like phases. New phase nanocrystallites can be prepared by polymerization of such molecules. Thus, the *TA*1, *TA*3, *TA*5, and *TA*6 phases can be obtained by polymerization of dimeric cyclo-octatetraene, whereas the *TA*2, *TA*4, *TA*7, *TA*8, and *TB* phases can be produced by polymerization of didehydrobiphenylenes. Using this method, apparently, it is impossible to obtain crystals of macroscopic sizes, since the number of stages in the procedure of synthesis quickly increases with new phase nanocrystallite sizes.

## Conclusions

In the present paper, the structures and properties of carbon diamond-like *T*- and *S*-phases were theoretically investigated. Nine *T*-phases can be obtained in the process of linking or combining SWCNTs. The structures of four *S*-phases are formed by internally linking three-dimensional graphites. Two new diamond polymorphs, namely *SA*3 and *SA*4 phases, were investigated for the first time. For all phases, various structural parameters, cohesive energies, bulk moduli, hardness, electron densities of states, and powder XRD patterns were calculated.

Carbon materials formed on the basis of the majority of *T*-and *S*-phases should be dielectric materials because their band gap values calculated using the GGA-DFT method are larger than 2.4 eV. Only the *TA*1 phase is a semiconductor with a small band gap of 1.31 eV comparable to the corresponding value for silicone (1.11 eV [28]). All diamond-like *T*- and *S*-phases should have high strength properties; therefore, they can be used for developing new abrasive and constructional materials. The calculated XRD patterns of *T*- and *S*-phases can be applied to identify these phases in synthesized carbon materials. The XRD patterns of *SA*1, *SA*2, and nine *T*-phases sufficiently strongly differ from those of cubic diamond, lonsdaleite, and 2*H* graphite, and therefore their identification should not cause difficulties; whereas new *SA*3 and *SA*4 phases can only be identified based on secondary diffraction maxima.

## References


1. Robertson J (1991) Hard amorphous (diamond-like) carbons. Prog Solid State Chem 21:199–333
2. Belenkov EA, Greshnyakov VA (2013) Classification schemes of carbon phases and nanostructures. New Carbon Mater 28: 273–283
3. Lord EA, Mackay AL, Ranganathan S (2006) New geometries for new materials. Cambridge University Press, Cambridge
4. Radushkevich LV, Luk'yanovich VM (1952) The structure of carbon forming in thermal decomposition of carbon monoxide on an iron catalyst (in Russian). Sov J Chem Phys 26:88–95. http://nanotube.msu.edu/HSS/2006/4/2006-4.pdf
5. Davis WR, Slawson RJ, Rigby GR (1953) An unusual form of carbon. Nature 171:756
6. Iijima S (1991) Helical microtubules of graphitic carbon. Nature 354:56–58
7. Cao L, Gao C, Sun H, Zou G, Ze Zhang, Zhang X, He M, Zhang M, Li Y, Zhang J, Dai D, Sun L, Wang W (2001) Synthesis of diamond from carbon nanotubes under high pressure and high temperature. Carbon 39:311–314
8. Zhang F, Shen J, Sun J, McCartney DG (2006) Direct synthesis of diamond from low purity carbon nanotubes. Carbon 44:3136–3138
9. Reich S, Ordejon P, Wirth R, Maultzsch J, Wunder B, Muller H-J, Lathe C, Schilling F, Dettlaff-Weglikowska U, Roth S, Thomsen C (2003) Hexagonal diamond from single-walled carbon nanotubes. AIP Conf Proc 685:164–168
10. Wang Z, Zhao Y, Tait K, Liao X, Schiferl D, Zha C, Downs RT, Qian J, Zhu Y, Shen T (2004) A quenchable superhard carbon phase synthesized by cold compression of carbon nanotubes. Proc Natl Acad Sci USA 101:13699–13702
11. Popov M, Kyotani M, Koga Y (2003) Superhard phase of single wall carbon nanotube: comparison with fullerite $C_{60}$ and diamond. Diam Relat Mater 12:833–839
12. Khabashesku VN, Gu Z, Brinson B, Zimmerman JL, Margrave JL, Davydov VA, Kashevarova LS, Rakhmanina AV (2002) Polymerization of single-wall carbon nanotubes under high pressures and high temperatures. J Phys Chem B 106:11155–11162
13. Liu D, Yao M, Li Q, Cui W, Bo Zou, Cui T, Liu B, Sundqvist B, Wagberg T (2011) High pressure and high temperature induced polymerization of $C_{60}$ nanotubes. CrystEngComm 13:3600–3605
14. Baughman RH, Galvao DS (1993) Tubulanes: carbon phases based on cross-linked fullerene tubules. Chem Phys Lett 211: 110–118
15. Domingos HS (2004) Carbon allotropes and strong nanotube bundles. J. Phys 16:9083–9091

16. Hu M, Zhao Z, Tian F, Oganov AR, Wang Q, Xiong M, Fan C, Wen B, He J, Yu D, Wang H-T, Bo Xu, Tian Y (2013) Compressed carbon nanotubes: a family of new multifunctional carbon allotropes. Sci Rep 3:1331
17. Omata Y, Yamagami Y, Tadano K, Miyake T, Saito S (2005) Nanotube nanoscience: a molecular-dynamics study. Physica E 29:454–468
18. Zhao Z, Bo Xu, Zhou X-F, Li-M Wang, Wen B, He J, Liu Z, Wang H-T, Tian Y (2011) Novel superhard carbon: c-centered orthorhombic $C_8$. Phys Rev Lett 107:215502
19. Zhao ZS, Zhou X-F, Hu M, Yu DL, He JL, Wang H-T, Tian YJ, Xu B (2012) High-pressure behaviors of carbon nanotubes. J Superhard Mater 34:371–385
20. Belenkov EA, Greshnyakov VA (2014) New structural modifications of diamond: LA9, LA10, and CA12. J Exp Theor Phys 119:101–106
21. Giannozzi P, Baroni S, Bonini N, Calandra M, Car R, Cavazzoni C, Ceresoli D, Chiarotti GL, Cococcioni M, Dabo I, Corso AD, de Gironcoli S, Fabris S, Fratesi G, Gebauer R, Gerstmann U, Gougoussis C, Kokalj A, Lazzeri M, Martin-Samos L, Marzari N, Mauri F, Mazzarello R, Paolini S, Pasquarello A, Paulatto L, Sbraccia C, Scandolo S, Sclauzero G, Seitsonen AP, Smogunov A, Umari P, Wentzcovitch RM (2009) QUANTUM ESPRESSO: a modular and open-source software project for quantum simulations of materials. J Phys 21:395502
22. Becke AD (1993) Density-functional thermochemistry. III. The role of exact exchange. J Chem Phys 98:5648–5652
23. Greshnyakov VA, Belenkov EA (2014) Technique for calculating the bulk modulus. Russ Phys J 57:731–737
24. Gao F, He J, Wu E, Liu S, Yu D, Li D, Zhang S, Tian Y (2003) Hardness of covalent crystals. Phys Rev Lett 91:015502
25. Li K, Wang X, Zhang F, Xue D (2008) Electronegativity identification of novel superhard materials. Phy Rev Lett 100:235504
26. Guinier A (1964) Theorie et technique de la radiocristallographie. A. Dunod, Paris
27. Belenkov EA, Greshnyakov VA (2015) Diamond-like phases prepared from graphene layers. Phys Solid State 57:205–212
28. Kittel C (1996) Introduction to solid states physics, 7th edn. Wiley, New York
29. Johnston RL, Hoffmann R (1989) Superdense carbon, $C_8$: supercubane or analogue of $\gamma$-Si? J Am Chem Soc 111:810–819
30. Andrievski RA (2001) Superhard materials based on nanostructured high-melting point compounds: achievements and perspectives. Int J Refract Met Hard Mater 19:447–452
31. Brookes CA, Brookes EJ (1991) Diamond in perspective: a review of mechanical properties of natural diamond. Diamond Relat Mater 1:13–17
32. Swanson HE, Fuyat RK (1953) Standard X-ray diffraction powder patterns. National Bureau of Standards circular, 539, vol II. National Bureau of Standards, Washington, DC, p 5
33. Bundy FP, Kasper JS (1967) Hexagonal diamond—a new form of carbon. J Chem Phys 46:3437–3446
34. Sanc I (1990) Pattern: 00-041-1478. Graphite-2H, polytechna. ICDD Grant-in-Aid, Foreign Trade Corporation, Panska, Czechoslovakia
35. Metha G, Viswanath MB, Sastry GN, Jemmis ED, Reddy DSK, Kunwar AC (1992) Quest for higher ladderanes: oligomerization of a cyclobutadiene derivative. Angew Chem Int Ed Engl 31:1488–1490
36. Katz TJ, Acton N (1973) Synthesis of prismane. J Am Chem Soc 95:2738–2739
37. Eaton PE, Cole TW Jr (1964) The cubane system. J Am Chem Soc 86:962–964
38. Eaton PE, Or YS, Branca SJ (1981) Pentaprismane. J Am Chem Soc 103:2134–2136
39. Wiberg KB, Matturro MG, Okarma PJ, Jason ME (1984) Tricyclo[4.2.2.$2^{2,5}$]dodeca-1,5-diene. J Am Chem Soc 106:2194–2200
40. Hoffmann VT, Musso H (1987) Nonacyclo[10.8.0.$0^{2,11}$.$0^{4,9}$.$0^{4,19}$.$0^{6,17}$.$0^{7,16}$.$0^{9,14}$.$0^{14,19}$]-icosane, a double tetraasterane. Angew Chem Int Ed Engl 26:1006–1007
41. Ternansky RJ, Balogh DW, Paquette LA (1982) Dodecahedrane. J Am Chem Soc 104:4503–4504
42. Geim AK, Novoselov KS (2007) The rise of graphene. Nat Mater 6:183–191
43. Zhao X, Liu Y, Inoue S, Suzuki T, Jones RO, Ando Y (2004) Smallest carbon nanotube is 3 Å in diameter. Phys Rev Lett 92:125502
44. Guan L, Suenaga K, Iijima S (2008) Smallest carbon nanotube assigned with atomic resolution accuracy. Nano Lett 8:459–462
45. Peng L-M, Zhang ZL, Xue ZQ, Wu QD, Gu ZN, Pettifor DG (2000) Stability of carbon nanotubes: how small can they be? Phys Rev Lett 85:3249–3252
46. Sun LF, Xie SS, Liu W, Zhou WY, Liu ZQ, Tang DS, Wang G, Qian LX (2000) Creating the narrowest carbon nanotubes. Nature 403:384
47. Rols S, Goncharenko IN, Almairac R, Sauvajol JL, Mirebeau I (2001) Polygonization of single-wall carbon nanotube bundles under high pressure. Phys Rev B 64:153401
48. Braga SF, Galvao DS (2006) Single wall carbon nanotubes polymerization under compression: an atomistic molecular dynamics study. Chem Phys Lett 419:394–399
49. Kosakovskaya ZYA, Chernozatonskii LA, Fedorov EA (1992) Nanofilament carbon structure. JETP Lett 56:26–30
50. Krasheninnikov AV, Nordlund K, Keinonen J, Banhart F (2002) Ion-irradiation-induced welding of carbon nanotubes. Phys Rev B 66:245403
51. Bundy FP, Bassett WA, Weathers MS, Hemley RJ, Mao HK, Goncharov AF (1996) The pressure-temperature phase and transformation diagram for carbon; updated through 1994. Carbon 34:141–153